International Journal of Heat and Technology
Vol. 44, No. 2, April, 2026, pp. 591-601
Journal homepage: http://iieta.org/journals/ijht

Heat Transfer Enhancement Using Twisted Tape Inserts: A Comparative Study Between Triangular and Rectangular Cross-Sections

Farah Abd-Alsalam Ibrahim[1,2*], Nabil Jamil Yasin[3], Tahseen Ali Jabbar[2]

[1] Department of Thermal Mechanical Engineering, Engineering Technical College-Baghdad, Middle Technical University, Baghdad 10001, Iraq
[2] Department of Thermal Mechanical Engineering, Engineering Technical College-Basra, Southern Technical College, Basra 61001, Iraq
[3] Department of Mechanical Engineering, Al-Amarah University College, Al-Amarah 62001, Iraq

Corresponding Author Email: farah.abdalsalam@stu.edu.iq

https://doi.org/10.18280/ijht.440213

Received: 15 January 2026
Revised: 11 April 2026
Accepted: 24 April 2026
Available online: 30 April 2026

Keywords:
triangular twisted tape, Reynolds number, thermal performance, equal cross section area, equal surface area

ABSTRACT

Enhancing heat transfer in thermal systems is important for increasing energy savings and low cost. This study numerically investigates heat transfer enhancement (HTE) using triangular twisted tape (TTT) inserts and compares their performance with rectangular twisted tapes (RTT) of equivalent cross-sectional area and surface area. The analysis was conducted over a range of base-to-height ratios (b/h) of the TTT varying from 0.35 to 3.85. ANSYS Fluent simulations were carried out for a 508 mm long and 31.75 mm diameter circular tube with a twist ratio of 1.57. The working fluid used was air, and a constant heat flux of 8000 W/m² with Reynolds numbers 5000-25,000. Results show that for a b/h ratio of 0.35, TTT performs the best as a result of higher turbulence intensity and better fluid mixing to decrease temperature gradients, while for larger b/h the turbulence gets weaker. For the constant cross-sectional area configuration, triangular tapes are significantly superior to rectangular ones, with an increase of about 25% and 17% improvement in thermal performance at Re 5000 and 25000, respectively, with significant increments in friction factor reaching 0.068. Even with the same tape surface area, triangular tapes still offer nearly 21% HTE with an increase in friction factor reaching 0.064 at Re 5000.

1. INTRODUCTION

Energy has become one of the most pressing issues facing humanity worldwide [1-3]. Heat exchangers (HEs) are extensively used in various industries and for a variety of applications such as petrochemical processing, power generation, aerospace engineering, and food engineering. There is also a lay role in energy recovery systems, particularly for the recovery of waste heat from internal combustion engines [4]. Therefore, improving the thermal performance of HEs is essential for reducing system size and operational costs. In addition, it decreased energy consumption and supports global efforts to mitigate climate change.

In recent years, various techniques have been proposed to enhance heat transfer. These techniques can be classified into three categories: active methods, passive methods, and hybrid methods. Active techniques require external energy input, such as acoustic waves or magnetic fields. Passive techniques operate without additional energy input, including the use of nanofluids, twisted tape (TT) inserts, and coiled wire inserts. Hybrid techniques, passive techniques that combine the advantages of both approaches [5-7]. Significant efforts have been devoted to the development and optimization of passive heat transfer enhancement (HTE) techniques aimed not only at improving the heat transfer rate but also at enhancing the overall thermo-hydraulic performance of HEs [8]. TT inserts are one of the most effective and practical passive HTE techniques, and it widely applied in engineering systems because it is favorable thermal performance, simple structure, ease of manufacturing and installation, and low manufacturing cost [9]. The mechanism induces swirling or secondary flow within the tube due to the insertion of TT, which enhances the mixing in the region near-wall fluid. Consequently, the thermal boundary layer is disrupted and increases in the turbulence intensity, leading to a significant enhancement in convective heat transfer performance without the need for additional external energy input [10]. Among the passive methods, TT inserts received extensive attention for their efficiency in improving the heat transfer performance of HEs. Many studies have been devoted to investigating whether and how the performance of TT inserts can be improved through geometric modifications and multi-tape configurations. For instance, Ponnada et al. [11] experimentally compared between Perforated twisted tapes with alternate axis (PATT), perforated twisted tapes (PTT) and conventional twisted tapes (CTT) under turbulent flow conditions. Their results showed that PATT provided the highest HTE, followed by PTT and TT. However, this improvement in thermal performance was accompanied by an increased friction factor (f).

Previously, Bhuiya et al. [12] presented Perforated Triple

Twisted Tape (PTTT) with varied porosities showing demanding rises in Nusselt number (Nu) reaching up to 320% when compared to a circular tube. However, this improvement came with a high cost and elevated pressure drop(ΔP), which suggested that there was a delicate balance between heat transfer and flow resistance.

Another study [13] also focused on the numerical investigation of single-cut and double-cut TTs. The researchers found that although double-cut configurations enhance heat transfer more effectively, higher-pressure losses were observed. Likewise, Chithra et al. [14] studied TT inserts in square ducts, and they found that even though the absolute value of heat transfer was lower with lesser friction penalties, shorter inserts turn out to be more thermally effective.

However, despite the abundance of investigations in this area, most studies have investigations have focused on conventional geometric shapes, including perforation or cuts and variations in tape length. In contrast, few attempts have been made to investigate the effect of TT cross-sectional shape. Especially non-rectangular geometries like triangular cross-sections are still not fully explored. Furthermore, previous studies did not provide systematic comparisons under controlled conditions, such as equal surface area or equal cross-sectional area, nor have they provided information on the optimum geometric parameters. Therefore, the present study systematically investigates the thermo-hydraulic performance and the effect of the geometric configuration of triangular twisted tape (TTT) inserts. The main objective is to determine the optimum b/h ratio value that achieves a maximum HTE with acceptable pressure drop. In addition, a comparison between TTT and rectangular twisted tapes (RTT) was conducted under the same conditions (equal surface area, equal cross-sectional area) to isolate the influence of geometry on flow pattern and heat transfer performance. This approach provides valuable insight into how geometric shape influences secondary flow structures, turbulence characteristics, and overall thermal performance.

2. MODEL DESCRIPTION

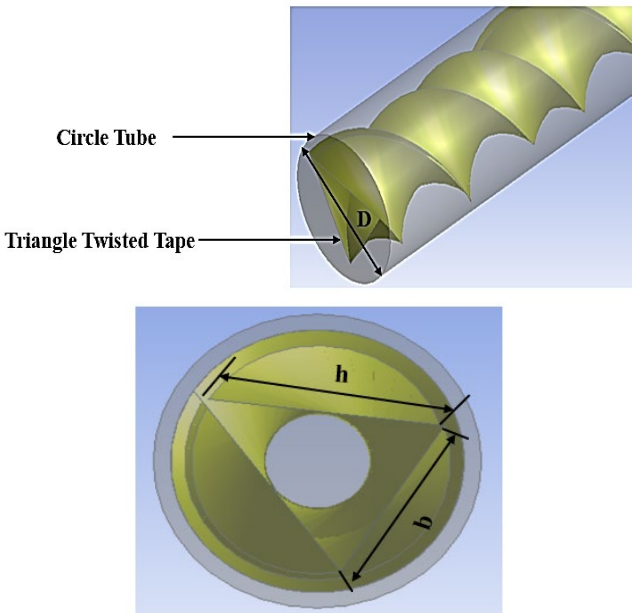

Figure 1. Physical geometry of a circular tube with triangular twisted tape (TTT)

The TTT was geometrically characterized by two main parameters: the base length (b) and the height (h). A range of base-to-height ratios (b/h = 0.35-3.85) was investigated to evaluate the effect of tape geometry on HTE and f characteristics inside a circular tube. The study was conducted in two major stages. In the first stage, the optimal b/h ratio for the TTT was identified through a series of numerical simulations performed using ANSYS Fluent. In the second stage, the thermo-hydraulic performance of the optimized TTT was compared with RTT. The comparison was carried out under equal cross-sectional area, equal surface area, and various Reynolds number (Re) [15]. The geometric configuration and coordinate system are presented in Figure 1. The test tube had a total length of 508 mm and an inner diameter of 31.75 mm. The Pitch (P) was kept constant at 50 mm for all cases, corresponding to a fixed twist ratio (TR = P/D = 1.57). Different b/h ratios of the TTT were simulated to assess their influence on thermo- hydraulic behavior under identical boundary and operating conditions.

3. MATHEMATICAL MODEL AND NUMERICAL METHOD

3.1 Governing equations

The investigated fluid flow is three-dimensional, incompressible, turbulent flow, and the steady-state behavior. The heat transfer processes are governed by the fundamental conservation equations, namely the continuity, Navier–Stokes, and energy equations as expressed below [16-18].

-Continuity equation

$$\frac{\partial u}{\partial x}+\frac{\partial u}{\partial y}+\frac{\partial u}{\partial z}=0 \tag{1}$$

-Momentum equation

In x-direction:

$$\rho\left(u\frac{\partial u}{\partial x}+v\frac{\partial u}{\partial y}+w\frac{\partial u}{\partial z}\right)=-\frac{\partial p}{\partial x}+\mu\left(\frac{\partial^2 u}{\partial x^2}+\frac{\partial^2 u}{\partial y^2}+\frac{\partial^2 u}{\partial z^2}\right) \tag{2}$$

In y-direction:

$$\rho\left(u\frac{\partial v}{\partial x}+v\frac{\partial v}{\partial y}+w\frac{\partial v}{\partial z}\right)=-\frac{\partial p}{\partial y}+\mu\left(\frac{\partial^2 v}{\partial x^2}+\frac{\partial^2 v}{\partial y^2}+\frac{\partial^2 v}{\partial z^2}\right) \tag{3}$$

In z-direction:

$$\rho\left(u\frac{\partial w}{\partial x}+v\frac{\partial w}{\partial y}+w\frac{\partial w}{\partial z}\right)=-\frac{\partial p}{\partial z}+\mu\left(\frac{\partial^2 w}{\partial x^2}+\frac{\partial^2 w}{\partial y^2}+\frac{\partial^2 w}{\partial z^2}\right) \tag{4}$$

- Energy equation

$$u\frac{\partial T}{\partial x}+v\frac{\partial T}{\partial y}+w\frac{\partial T}{\partial z}=\alpha\left(\frac{\partial^2 T}{\partial x^2}+\frac{\partial^2 T}{\partial y^2}+\frac{\partial^2 T}{\partial z^2}\right) \tag{5}$$

The (SST) k-ω turbulence model governing equations are as follows [19]:

The turbulence kinetic energy k:

$$\frac{\partial(ku_j)}{\partial x_j}=\frac{1}{\rho}.\frac{\partial}{\partial x_j}\{[\frac{\partial k}{\partial x_j}(\mu_l+\frac{\mu_t}{\sigma_k})]\}+\frac{G_k}{\rho}\varepsilon \tag{6}$$

where,

$$\mu_t = \rho C_\mu \frac{k^2}{\varepsilon}, G_k = 2\mu_t E_{ij}.E_{ij}, E_{ij} = \frac{1}{2}\{[\frac{\partial u_i}{\partial x_i} + \frac{\partial u_i}{\partial x_j}]\}$$

The constant for the current turbulent model is set as below [20]:

$$C_\mu = 0.09;\ C_{1\varepsilon} = 1.44;\ C_{2\varepsilon} = 1.92;\ \sigma_k = 1.0;\ \sigma_\varepsilon = 1.3$$

3.2 Data reduction

For the analyzed turbulent flow, the dimensionless parameters, namely the *f*, Re, heat transfer coefficient (h) and Nu were evaluated using the following mathematical expressions [21]:

$$h_{(x)} = \frac{q}{T_w - T_b} \quad (7)$$

where, T_w and T_b represented the wall temperature of heated tube and bulk temperature for fluid, respectively. As a result, enhancement of heat transfer depending on local Nusselt number ($Nu_{(x)}$) can be defined on [22]:

$$Nu_{(x)} = \frac{h(x)D}{k_f} \quad (8)$$

where, k_f thermal conductivity for air.

To calculate the average Nusselt number ($Nu_{average}$) [23]:

$$Nu_{\ average} = \frac{1}{L}\int_0^L Nu_{(x)}dx \quad (9)$$

The *Re* is defined as [24]:

$$Re = \frac{\rho u D}{\mu} \quad (10)$$

where, ρ density, u velocity of air, *D* diameter of tube and μ dynamic viscosity.

The Δp can be calculated by the equation [25]:

$$\Delta p = \frac{f L \rho u_m^2}{2D} \quad (11)$$

where, f: friction factor, u_m: the mean fluid velocity in the tube, *L*: the length of tube.

The HTE was quantified by the thermal performance factor (η) which depended on the comparison between a tube with and without TT inserts. It can be calculated using the following expression [26]:

$$\eta = (\frac{Nu_c}{Nu_p})(\frac{f_p}{f_c})^{\frac{1}{3}} \quad (12)$$

where, Nu_c, Nu_p, and f_c, f_p are Nu and *f* with and without TT in tube, respectively.

The *Nu* and *f* for the tube without a twist can be calculated from [27]:

Dittus–Boelter correlation for turbulent flow:

$$Nu = 0.023\ Re^{0.8}\ Pr^{1/3} \quad (13)$$

Correlation of Gnielinski:

$$Nu = \frac{(f/8)(Re-1000)Pr}{1+12.7\left(\frac{f}{8}\right)^{1/2}(Pr^{1/3}-1)} \quad (14)$$

Blasius equation for turbulent flow:

$$f = 0.079\ Re^{-0.25} \quad (15)$$

Correlation of Petukhov:

$$f = (0.79lnRe - 1.64)^{-2} \quad (16)$$

3.3 Boundary condition

In the present work, it focused on air as a working fluid and the thermophysical properties of air are constant in all the Computational Fluid Dynamics (CFD) simulations. The inlet velocity was determined to obtain a Re of 5,000–25,000 as required for the study and the inlet temperature (T_1) was fixed at 300 K supplemented with a pressure outlet condition on the tube exit. The tube wall is uniformly heated by a heat flux of about 8000 W/m² to introduce the same thermal load on it. A no-slip boundary condition is employed at all solid walls, which include the inner wall of the tube and TT surfaces. The air properties used in the analysis are given as under: Density (1.225 kg/m^3), Specific heat at constant pressure (Cp = 1006.43 J/kg·K), the thermal conductivity (K = 0.0242 W/m·K) and the dynamic viscosity (μ = 0.0000178 kg/m·s) [28].

3.4 Numerical method

The CFD simulations were performed by using Ansys Fluent 2020 to solve the governing equations and associated boundary conditions in numerical algorithms within a suitable computational domain. The governing equation is discretized and solved using the finite volume method (FVM) with the given boundary conditions. The SST k-ω turbulence model is employed to simulate turbulence effects because of its capability to accurately predict near-wall flows, and provide accurate predictions of flow separation and swirling motion. This model is especially applicable to internal flows with increased turbulence intensity induced by TT inserts. Furthermore, the SST k-ω model is widely used in previous numerical investigations of TT geometries, and it demonstrated good agreement with experimental and numerical results [29-31]. Medium mesh resolution and second-order upwind discretization schemes are applied for momentum and energy equations. Convergence is assumed when the residuals for continuity, velocity, and energy fall below 10^{-6}.

3.5 Grid independence

Mesh sensitivity analyses were conducted to ensure that the numerical results were independent of the mesh density. The computational grid was progressively refined until reaching no noticeable variation in the computed quantities. Due to the geometric complexity of the domain, an unstructured tetrahedral mesh was employed. In addition, 20 inflation layers were generated near the tube wall to accurately resolve the velocity and temperature gradients within the boundary layer. Figure 2 illustrates the overall computational mesh refined regions and the surface mesh employed in the three-dimensional simulations with non-uniform mesh distribution. A grid independence test at Re = 5000 was run by using the *Nu* and *f* as shown in Table 1. Both *Nu* and *f* are seen to increase with mesh refinement yet converge towards a stable

value at larger element counts. At some grid size the difference between consecutive meshes becomes negligible, which means that the result is mesh-independent. As a result, the selected mesh has given valid and accurate predictions.

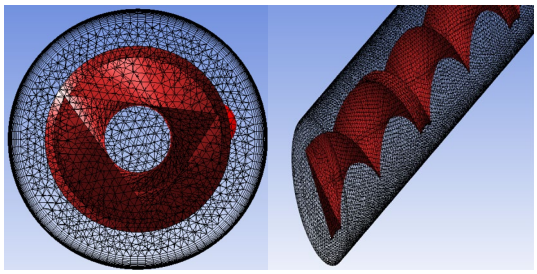

Figure 2. The structure mesh

Table 1. Grid independent study

Number of Elements	Nu	*f*
1081268	34.27722436	0.062127108
1235424	35.94416177	0.062835987
1481268	38.63749492	0.064057255
1616735	39.14368299	0.064803606
1899426	40.02515244	0.065918331
2026081	41.47877394	0.066982909
2288562	42.69822224	0.067617218
2422485	43.53708318	0.068643486
2612139	43.89644294	0.068637986
2842551	43.9084344	0.068618971

3.6 Validation

In order to validate the present numerical model, a comparison between Nu and *f* with the numerical results reported by Cabello [32] for TT at Re from 5000 to 25000, as illustrated in Figures 3 and 4. The present numerical predictions showed good agreement with the reference data across of Re for both Nu and *f*. The deviation between the present results and the reference data is within 5%. These minor differences may be attributed to variations in boundary conditions, geometric simplifications and the mesh resolution used for discretizing the governing equations.

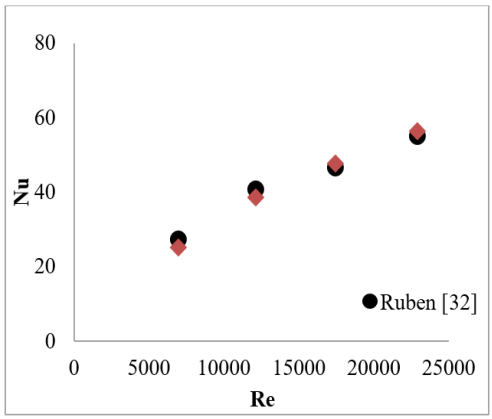

Figure 3. Validation of Nu with result [32]

The variation of the Nu and *f* with Re is presented in Figures 5 and 6. Among the considered correlations, the Gnielinski equation predicted the highest Nu values, followed by the Dittus–Boelter correlation. In contrast, the present numerical simulations on a plain tube produced slightly lower values. This deviation is expected because the Gnielinski correlation considers the *f* and generally provides high accuracy with turbulent flow conditions. However, for all the cases considered, Re increased and *f* decreased with increasing Re in the smooth tube under turbulence flow. In addition, Blasius correlation slightly underestimated the *f* in comparison with the updated numerical results, while Petukhov equation showed closer agreement with the present study. It should be noted that the present numerical predictions showed good agreement with a set of empirical correlations. The deviations between present results and the correlations remain within an acceptable limit at a maximum error not cross about 5% for Nu and about 3% for *f*. These discrepancies are due to the use of different turbulence models, boundary conditions, simplifying geometries and numerical discretization methods.

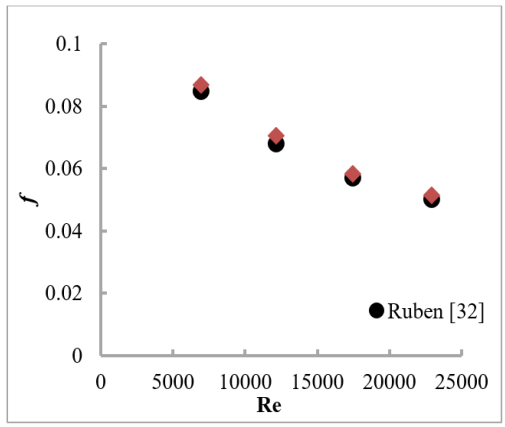

Figure 4. Validation *f* with result [32]

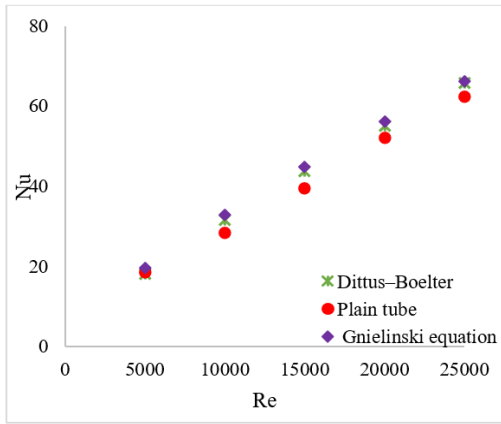

Figure 5. Confirmation of Nu for plain tube

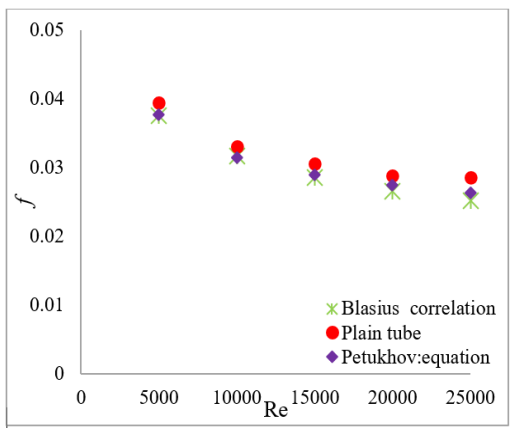

Figure 6. Confirmation of *f* for plain tube

4. RESULT AND DISCUSSION

In this study, the influence of TTT inserts with a range of ratios (b/h = 0.35-3.85) on heat transfer performance was investigated. The results showed that the Nu was significantly enhanced at an optimal b/h ratio while the *f* remains within an acceptable range. Figure 7 illustrates the variation of Nu with b/h for the TTT insert, indicating that the heat transfer performance is strongly dependent on tape geometry. The rate of increase in the Nu gradually reduces and remains nearly constant for b/h values above 0.6, followed by a slight increase at higher ratios.

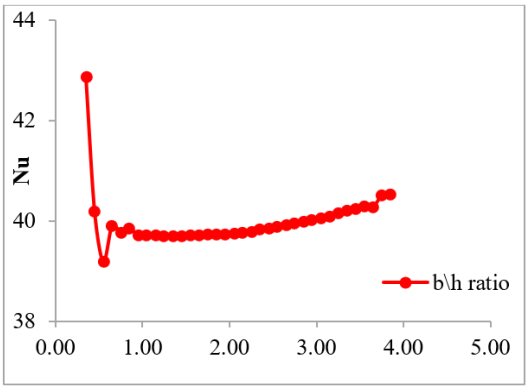

Figure 7. Distribution of Nu for different b/h ratios triangular twisted tape (TTT) at Re 5000

At a low b/h ratio, the slender triangular tape obstructs a larger portion of the flow area. It made two strong swirling vortices along the tube. This structure of flow leads to enhanced turbulent kinetic energy in the near-wall region and continuously disrupts the thermal boundary layer, which is a key contributor to HTE instead of simple fluid mixing. In addition, these vortices promote intermixing of the fluids between the core and the fluid near the wall, leading to better convective heat transfer. Furthermore, the sharp triangular tip acts as a flow splitter, which repeatedly disrupts the thermal boundary layer and thereby significantly enhances heat transfer. On the other hand, at higher b/h ratios, flatter triangular geometries are formed on the tape, resulting in reduced flow obstruction, weaker swirl generation, and a lower velocity gradient near the wall region. Consequently, thermal boundary layers become thicker and reduction in convective heat transfer. Moreover, the reduction in the shear stress and flow impingement decreases turbulence generation and leads to the observed decline in the Nu.

The Nu shows a recovery trend at higher ratios (b/h > 3.0), with the difference being marginally observed. This behavior may be attributed to the reduction of recirculation zones and pressure drop losses, resulting in a better uniform flow and heat transfer stabilization. The smoother geometry at this location permitted a reattachment of the flow along the wall, and it enhanced the effective area of heat transfer. This behavior can be explained by the balance between reduced flow separation and improved flow reattachment, which stabilizes the thermal boundary layer development along the tube wall. Overall, the results indicate that best the highest of transfer is observed at small values of b/h ratios, approximately 0.35–0.4, where a combination of strong swirl flow and higher turbulence levels leads to maximum Nu enhancement.

Figure 8 presents the variation of *f* and turbulence intensity trend with a dimensionless ratio b/h at Re = 5000. The results indicate that the flow behavior can be classified into three regions. In the first region ($0.35 \leq b/h \leq 1.35$), the *f* decreases gradually from about 0.053, and turbulence intensity is nearly constant at about 36–40%. This behavior relatively stable flow with a moderate level of turbulence flow regime. A significant increase in turbulence intensity (approximately 54%) corresponding to the second region ($1.45 \leq b/h \leq 2.55$) represents a high flow disturbance induced by the geometric configuration. This part of the region has a higher *f,* which means greater energy dissipation due to enhanced turbulence and mixing. However, the turbulence intensity decreased again in the region ($3.5 \leq b/h < 4$) where it stabilizes at around 36% while f increases gradually, exceeding 0.05. The results demonstrate that the b/h ratio is the dominant turbulence behavior and frictional losses. Although higher turbulence levels enhance mixing and improve heat transfer, but it led to an increase in ΔP, which creates a trade-off between thermal performance and hydraulic losses. Accordingly, geometry configuration at ratio b/h = 0.35 provides the most favorable balance of enhanced heat transfer with acceptable hydraulic resistance, and this configuration proved the optimum case among all investigated ratios.

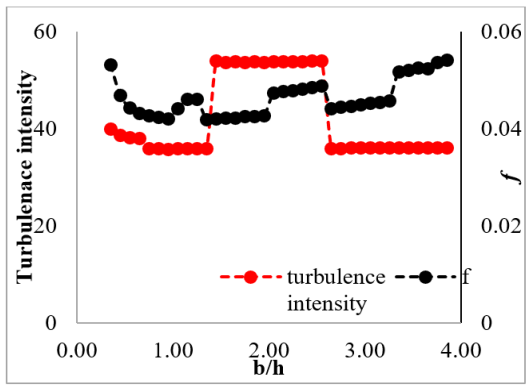

Figure 8. Turbulence intensity and *f* distribution for different b/h ratios of triangular twisted tape (TTT) at Re 5000

The static temperature distribution in the tube with TTT inserts at different ratios of b/h is shown in Figure 9. The results indicate that the geometry significantly influences the thermal performance. The case of b/h = 0.35 shows a more uniform temperature distribution, indicating stronger secondary flow and enhanced heat transfer.

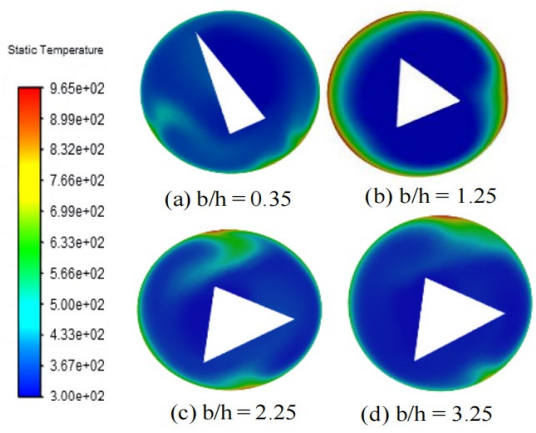

Figure 9. Static temperature field at various b/h ratios of triangular twisted tape (TTT) in the tube

On the other hand, lower ratios provided low heat transfer rates, but higher ratios produced high-pressure losses. Consequently, b/h = 0.35 represented the optimum configuration as it provides a good HTE with an admissible hydraulic resistance.

Contour plots of turbulent intensity for TTT at various ratios are shown in Figure 10 inside a circular tube. The results indicate that the turbulent intensity decreases gradually increases the ratio from 0.35 to 3.25. At b/h = 0.35, the highest turbulence is generated due to the sharp triangular edges, which generate strong swirl flow and enhance interaction between the core flow and near-wall fluid region. This enhancement is mainly driven by strong shear layer development and continuous disruption of the thermal boundary layer. For b/h = 1.25 and 2.25, the flow becomes relatively more stable with smaller-scale vortices and weaker turbulence intensity, resulting in reduced convective mixing effectiveness. At higher ratios, the flow becomes almost uniform with minimal agitation due to the smoother triangular geometry, which reduces blockage and rotational effects. Overall, the ratio b/h = 0.35 configuration demonstrates the best thermal performance since it triggers the highest turbulence intensity and vortex strength among all cases, resulting in a significant improvement in convective heat transfer compared with other configurations.

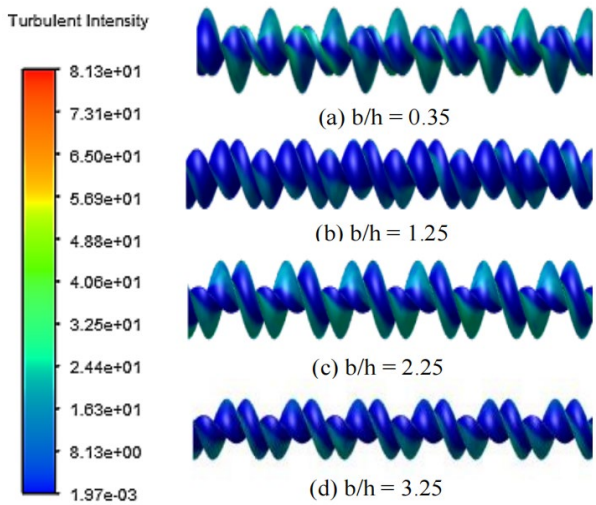

Figure 10. Triangular twisted tape (TTT) ratio effects on turbulence intensity of contour at various ratios

4.1 Comparison of the triangular twisted tape and rectangle twisted tape

This study compares the thermal and hydraulic performance of TTT and RTT under identical operating and geometric conditions. To ensure a fair comparison, both configurations were analyzed using the same tube length, diameter, pitch, and uniform wall heat flux. Two geometric constraints were applied: (i) equal cross-sectional area (ii) equal surface area for both tape configurations. The triangular tape was evaluated at its optimal ratio (b/h = 0.35), which was previously identified as the configuration providing the highest HTE while maintaining an acceptable ΔP. This configuration represents the condition where the overall thermos-performance efficiency is maximized. The objective of this comparison is to determine which tape geometry is more effective in enhancing heat transfer and to provide insight into their potential applicability in engineering systems.

4.1.1 Performance comparison under the same cross section area

To ensure a fair and rigorous comparison between the TTT and the RTT, both configurations were designed with an identical surface area of 71.439 mm² at the optimal ratio of b/h. This approach ensures that the effect of surface area is constant across all cases, allowing any observed differences to be attributed solely to the geometric shape and its ability to generate swirl and secondary flow structures. Maintaining the same surface area in both geometries provides a consistent basis for enhancing the effectiveness of configurations.

Figure 11 illustrates the variation of the η with Re for TTT and RTT. The results show an increase in the η reaching about 1.97 for TTT when compared with RTT, which has η of about 1.65 at Re 5000, corresponding to a performance improvement of nearly 20%. As Re 10000 and 25000, the η drops from 1.76 to 1.54 for TTT and 1.50 to 1.46 for RTTT, with a performance gain of about 17% to 12%, respectively. This behavior can be attributed to the stronger flow generated by TTT at lower Re numbers. The sharp edges of TTT generate strong vortical structures. Nevertheless, the TTT configuration continued to exhibit significantly superior thermo-hydraulic performance across all Re ranges.

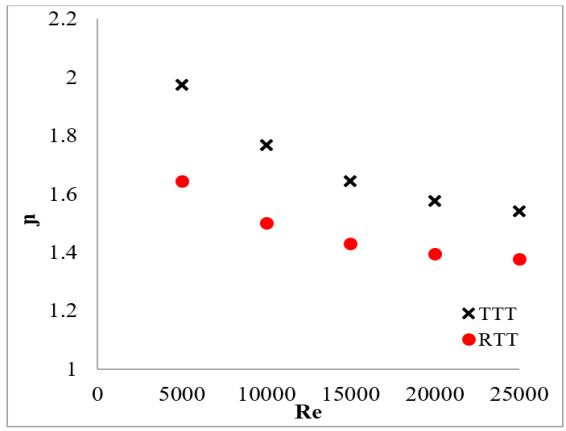

Figure 11. Thermal performance factor variation with Re for triangular twisted tape (TTT) and rectangular twisted tape (RTT) inserts at equal cross section area

The η is governed by the effect of Nu and *f*. The TT insertion in the tubes causes an increase in the Nu due to increased turbulence intensity, vortex generation, and improved radial mixing. However, the increase in f is associated with increased wall shear stress and flow resistance. Therefore, the η represented a balance between HTE and hydraulic losses. For TTT inserts, the results indicated that the enhancement in Nu is more than *f,* resulting in higher values η and improved overall thermo-hydraulic performance.

The present TTT configuration showed a higher η than other modified TT designs, such as single- cut and double-cut TTs, in a previous study [13]. The maximum η factor reaches approximately 2.19 while the corresponding values reported in the study [13] are about 1.45 and 1.7 single-cut and double-cut TTs, respectively, at Re 5000. These results indicate a significant enhancement in thermo-hydraulic performance for the TTT configuration.

Figure 12 illustrates the variation of Nu with Re for both TTT and RTT configurations. The results show the Nu

increases about 62 to 115 for TTT and 39 to 102 for RTT over the Re range 5000-25000 for both cases. This enhancement is attributed to the thinning of the thermal boundary layer and stronger turbulent transport with Re increase. The TTT configuration exhibited higher Nu than RTT for all ranges of Re. The sharp edges and tapering cross-section of the TTT geometry provided stronger longitudinal vortices and enhancing near-wall mixing and disturbing the thermal boundary layer.

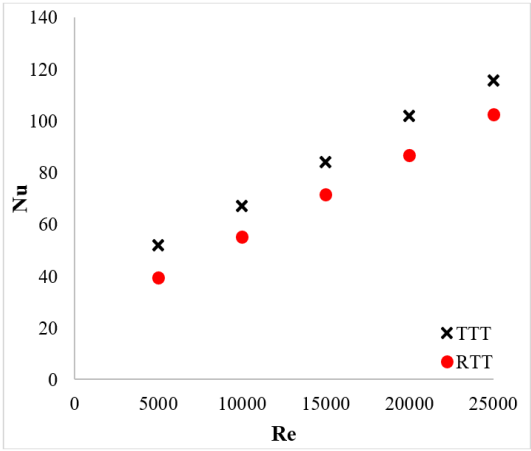

Figure 12. Variation of Nu with Re for triangular twisted tape (TTT) and rectangular twisted tapes (RTT) inserts at equal cross section area

Figure 13 illustrates the variation of *f* with Re for TTT and RTT configurations. Both configurations display gradually decrease in *f* as Re increases. This behavior is associated with the velocity of flow and inertial forces that increase over viscous forces. The results indicate that TTT produces higher f values than RTT at all Re ranges. The influence of geometry is clearly at lower Re where geometry-derived flow structures begin to dominate the behavior of these systems. As the Re increased, the difference in f between TTT and RTT because the flow becomes very turbulent and much less sensitive to geometric variations.

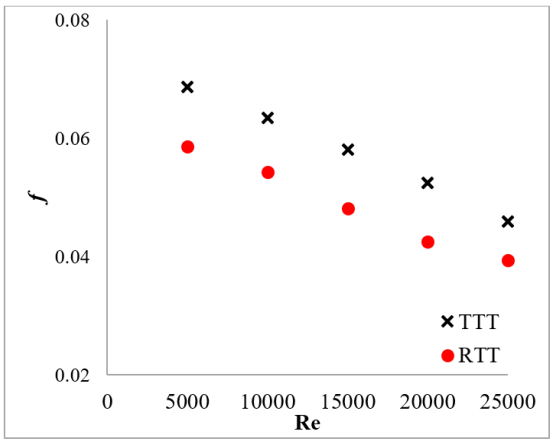

Figure 13. Variation of *f* with Re for triangular twisted tape (TTT) and rectangular twisted tapes (RTT) inserts at equal cross section area

This comparison provides main information about triangle and rectangle geometries that promote swirl flow, increase the degree of turbulence and influence the ΔP losses in the tube. Furthermore, the relationship between ΔP and Re was evaluated for the configurations to provide the surface effect combined with geometry induced flow disturbances enhances or leads to detriment in overall thermo-hydraulic effectiveness.

Figure 14 illustrates the variation of η with Re for both the TTT and RTT inserts under the same surface area condition. Both configurations show a gradual decrease in η with increasing Re, demonstrating that the impact of geometry induced swirl flow becomes weaker as the flow transitions to high turbulence conditions. The results show the evident improvement is more significant at lower Re to reach about 16% at Re 5000, but at Re 25000 reaches to 10% for TTT. This behavior is attributed to the stronger influence effected of secondary flows at low Re. Nevertheless, at higher Re TTT insert continues to have higher thermo-hydraulic performance compared with the RTT insert.

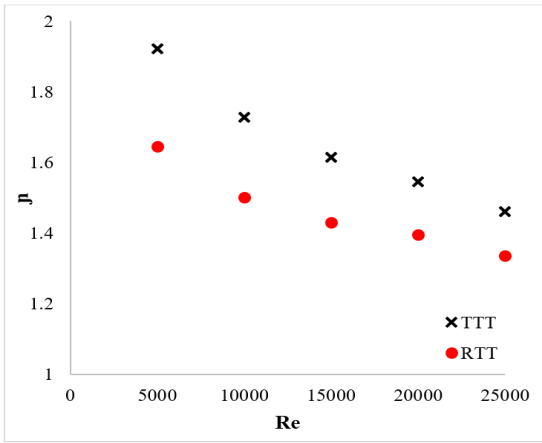

Figure 14. Variation η with Re for triangular twisted tape (TTT) and rectangular twisted tapes (RTT) inserts at constant surface area

4.1.2 Performance comparison under the same surface area

A comparison between TTT and RTT inserts was conducted, depending on a constant surface area of 53.626 mm. The purpose of this approach was to investigate the effect of tape geometry on flow and heat transfer. The configuration effect of the tape shape on pressure drops and thermal performance under fair conditions, when holding surface area constant at each value. Figure 15(a) and 15(b) illustrate the variation of Nu and *f* with Re for TTT and RTT configurations at constant surface area. For both configurations, the values of Nu increased with Re, as well as the *f* decreases with Re. This behavior can be ascribed to the stronger secondary flows and higher wall shear stress due to the sharper edges of triangular geometry. Figure 16 illustrates the variation of Nu with Re at constant surface area and cross-sectional area configuration. The result showed that Nu increases with increasing Re, demonstrating the greater convective heat transfer as flow turbulence intensifies. The cross-sectional area configuration generally yields higher Nu values than the surface area configuration. The difference between the two configurations remains relatively constant.

The cross-sectional area design consistently maintains an advantage under all operating conditions. The variation of *f* with Re, constant surface area and cross-sectional area configuration is represented in Figure 17. The configurations investigated highlight a clear thermo-hydraulic trade-off between enhancement of heat transfer and pressure loss. In

both cases, f decreases with increasing Re. The cross-sectional area configuration consistently yields higher f values reflecting its ability to promote more effective disruption of the thermal boundary layer.

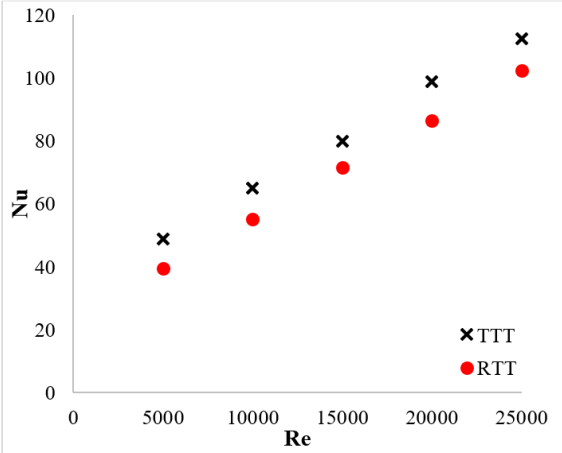

(a) Variation of the Nu with the Re

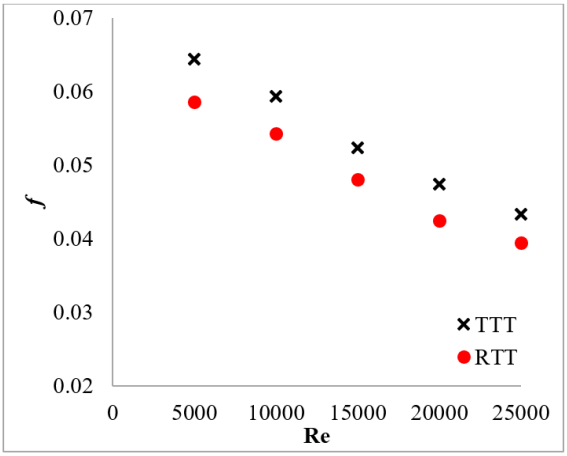

(b)Variation of the f with the Re

Figure 15. Compare between triangular twisted tape (TTT) and rectangular twisted tapes (RTT) inserts at constant surface area

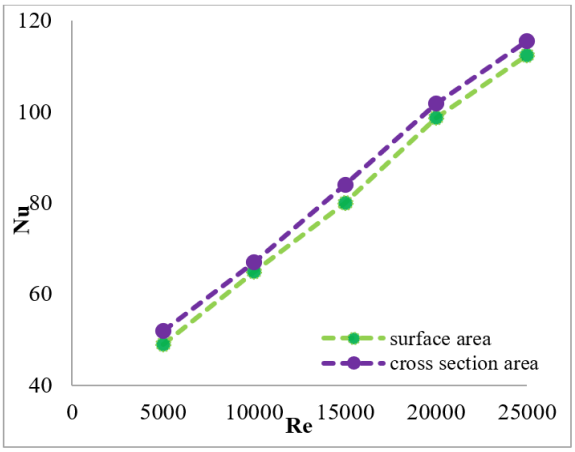

Figure 16. Variation of Nu with Re for equal surface area and equal cross-sectional area configurations

The flow behavior comparison between TTT and RTT configurations is represented in Figure 18. For the TTT configuration, the flow displays a clear and uniform swirling structure throughout the cross-section. The flow indicates the formation of strong secondary vortices, which enhance fluid mixing and reduce low-velocity regions as evidenced by the streamline patterns. In contrast, the flow structure becomes less uniform for the RTT. Streamlines are less smooth-looking with a visibly weak vortex and localized flow areas of low velocity, particularly surrounding the core region.

The differences are primarily attributed to the geometric properties of the inserts. The TTT with sharp edges promotes better disruption of the boundary-layer inducing higher turbulence and stronger vortex production. For an RTT, the flow disturbance is less strong. Thus, the improvement in heat transfer performance of the TTT is linked to improved mixing fluid and a thinner thermal boundary layer thickness that is consistent with higher Nu values.

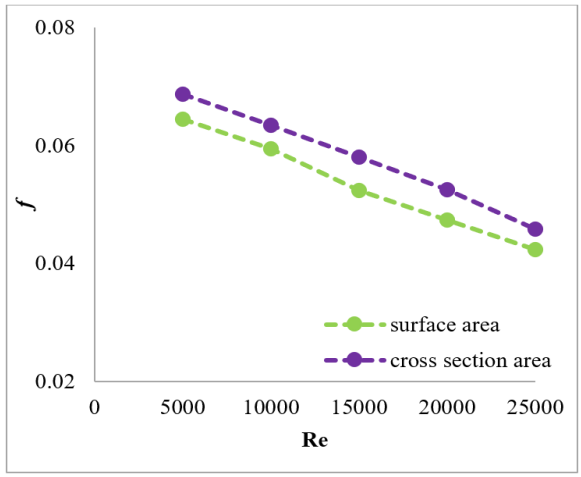

Figure 17. Variation in f with Re for equal surface area and equal cross-sectional area configurations

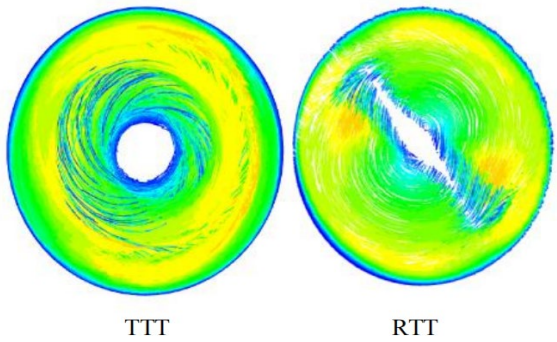

Figure 18. Velocity streamlines for Re = 5000
Note: triangular twisted tape (TTT); rectangular twisted tapes (RTT)

5. CONCLUSIONS

TT inserts are commonly used as passive HTE devices due to their ability to generate swirl flow, boundary layer separation, and significantly improve the performance of heat transfer without requiring external power. As tape geometry affects HTE and pressure drop, the understanding of their effects is significant in the optimization of thermal systems such as HEs and other energy-intensive processes. Therefore, this study investigates characterize and compares the thermo-hydraulic performance of TTT with different geometric parameters within tubular HEs relative to their counterpart

RTT under both constant surface area and cross-sectional area boundary conditions. The proposed TTT design is low-cost, easily manufactured, and fabricated for application as a passive internal component in conventional HE systems. The following are the main results of this study:

- The highest thermo-hydraulic performance of TTT is obtained at b/h = 0.35-0.40, where swirl intensity and turbulence are more pronounced. This condition enhances wall interaction and fluid mixing that contribute to uniform temperature distribution.

- Nu decreases from a ratio of 0.35 to around 0.6 and then remains almost constant with an increment in the b/h ratio. Both turbulence intensity and f decrease slowly with increasing in Re as the cross section of the tape expands and reduces disturbance flow.

- At constant cross section area, the TTT configuration exhibits a higher η of about 1.97 and 1.54 for TTT when compared with RTT configuration, about 1.64 and 1.33, respectively, and it is achieved from approximately 20% to 12% for Re 5000 and 25000, respectively. The thermos-hydraulic performance is mainly enhanced due to the sharper edges in the triangular geometry, which generate more strong swirl flow and an increase in fluid mixing, leading to a higher heat-transfer enhancement with a little increment of hydraulic resistance.

- At constant surface area, the TTT consistently outperforms the RTT across all Re. It achieves a maximum thermal performance factor of 1.92 at Re = 5000, about 17 % higher than the RTT and maintains superior Nu with enhancements ranging from 19% to 10% across Re = 5000 – 25,000. Although the TTT results in moderately higher *f* about 18–12% compared to the RTT, the substantial improvement in heat transfer ensures a superior overall thermo-hydraulic performance.

REFERENCES

[1] Riaz, F., Yam, F.Z., Qyyum, M.A., Shahzad, M.W., Farooq, M., Lee, P.S., Lee, M. (2021). Direct analytical modeling for optimal, on-design performance of ejector for simulating heat-driven systems. Energies, 14(10): 2819. https://doi.org/10.3390/en14102819

[2] Rezazadeh, R., Jafarmadar, S., Khorasani, S., Niaki, S.R.A. (2022). Experimental investigation on thermal behavior of non-boiling slug and bubbly two phase-flow in helical tube with spiral. Proceedings of the Institution of Mechanical Engineers, Part C: Journal of Mechanical Engineering Science, 236(7): 3434-3446. https://doi.org/10.1177/0954406221104204

[3] Riaz, F., Tan, K.H., Farooq, M., Imran, M., Lee, P.S. (2020). Energy analysis of a novel ejector-compressor cooling cycle driven by electricity and heat (waste heat or solar energy). Sustainability, 12(19): 8178. https://doi.org/10.3390/su12198178

[4] Luo, J., Alghamdi, A., Aldawi, F., Moria, H., Mouldi, A., Loukil, H., Deifalla, A.F., Ghoushchi, S.P. (2024). Thermal-frictional behavior of new special shape twisted tape and helical coiled wire turbulators in engine heat exchangers system. Case Studies in Thermal Engineering, 53: 103877. https://doi.org/10.1016/j.csite.2023.103877

[5] Hayat, M.Z., Nandan, G., Tiwari, A.K., Sharma, S.K., Shrivastava, R., Singh, A.K. (2021). Numerical study on heat transfer enhancement using twisted tape with trapezoidal ribs in an internal flow. Materials Today: Proceedings, 46: 5412-5419. https://doi.org/10.1016/j.matpr.2020.09.061

[6] Maleki, N.M., Ameri, M., Khoshkhoo, R.H. (2022). Experimental and numerical study of the thermal-frictional behavior of a horizontal heated tube equipped with a vibrating oscillator turbulator. International Communications in Heat and Mass Transfer, 135: 106154. https://doi.org/10.1016/j.icheatmasstransfer.2022.106154

[7] Garg, M.O., Nautiyal, H., Khurana, S., Shukla, M.K. (2016). Heat transfer augmentation using twisted tape inserts: A review. Renewable and Sustainable Energy Reviews, 63: 193-225. https://doi.org/10.1016/j.rser.2016.04.051

[8] Promvonge, P., Promthaisong, P., Skullong, S. (2020). Experimental and numerical heat transfer study of turbulent tube flow through discrete V-winglets. International Journal of Heat and Mass Transfer, 151: 119351. https://doi.org/10.1016/j.ijheatmasstransfer.2020.119351

[9] Bas, H., Ozceyhan, V. (2012). Heat transfer enhancement in a tube with twisted tape inserts placed separately from the tube wall. Experimental Thermal and Fluid Science, 41: 51-58. https://doi.org/10.1016/j.expthermflusci.2012.03.008

[10] Kiros, A.K., Tewolde, D.G., Atsbeha, A.K., Gebru, K.G., Teklehaimanot, T.T. (2025). Effect of multi-leg twisted tape inserts on heat transfer and pressure drop characteristics of a laminar pipe flow: A comparative analysis. Case Studies in Thermal Engineering, 74: 106838. https://doi.org/10.1016/j.csite.2025.106838

[11] Ponnada, S., Subrahmanyam, T., Naidu, S.V. (2019). A comparative study on the thermal performance of water in a circular tube with twisted tapes, perforated twisted tapes and perforated twisted tapes with alternate axis. International Journal of Thermal Sciences, 136: 530-538. https://doi.org/10.1016/j.ijthermalsci.2018.11.008

[12] Bhuiya, M.M.K., Roshid, M.M., Talukder, M.M.M., Rasul, M.G., Das, P. (2020). Influence of perforated triple twisted tape on thermal performance characteristics of a tube heat exchanger. Applied Thermal Engineering, 167: 114769. https://doi.org/10.1016/j.applthermaleng.2019.114769

[13] Nashee, S.R. (2024). Numerical simulation of heat transfer enhancement of a heat exchanger tube fitted with single and double-cut twisted tapes. International Journal of Heat and Technology, 42(3): 1003-1010. https://doi.org/10.18280/ijht.420327

[14] Chithra, V.P., Bakthavatchalam, B., Jayakumar, V., Kusekar, S., Pandey, A.K., Habib, K., Algarni, S., Alqahtani, T. (2025). Enhancing heat transfer in compound twisted square ducts using shortened twisted tape inserts. Results in Engineering, 26: 104862. https://doi.org/10.1016/j.rineng.2025.104862

[15] Ibrahim, F.A.A., Yasin, N.J., Jabbar, T.A. (2026). Effect of the width-diameter ratio of twisted tape inserts in heat exchanger tubes on heat transfer. ASEAN Journal for Science and Engineering in Materials, 5(1): 177-196.

[16] Kalash, A.R., Yasin, N.J. (2024). Experimental and computational assessment of the heat transfer exchange

in evacuated tube receiver using helical external fins. International Journal of Thermofluids, 24: 100963. https://doi.org/10.1016/j.ijft.2024.100963
[17] Qasim, R.M., Jabbar, T.A., Faisal, S.H. (2022). Effect of the curved vane on the hydraulic response of the bridge pier. Ocean Systems Engineering, 12(3): 335-358. https://doi.org/10.12989/ose.2022.12.3.335
[18] Murugesan, P., Mayilsamy, K., Suresh, S., Srinivasan, P.S.S. (2011). Heat transfer and pressure drop characteristics in a circular tube fitted with and without V-cut twisted tape insert. International Communications in Heat and Mass Transfer, 38(3): 329-334. https://doi.org/10.1016/j.icheatmasstransfer.2010.11.010
[19] Abdulrahman, R.S., Ibrahim, F.A., Faisel, S.H. (2020). Numerical study of heat transfer and exergy analysis of shell and double tube heat exchanger. International Journal of Heat and Technology, 38(4): 925-932. https://doi.org/10.18280/ijht.380419
[20] You, Y., Chen, Y., Xie, M., Luo, X., Jiao, L., Huang, S. (2015). Numerical simulation and performance improvement for a small size shell-and-tube heat exchanger with trefoil-hole baffles. Applied Thermal Engineering, 89: 220-228. https://doi.org/10.1016/j.applthermaleng.2015.06.012
[21] Sedaghat, R., Dalili, K.M., Hosseinalipour, S.M. (2024). A comprehensive analysis of heat transfer in a heat exchanger with simple and perforated twisted tapes based on numerical simulations. Case Studies in Thermal Engineering, 56: 104227. https://doi.org/10.1016/j.csite.2024.104227
[22] Ghalambaz, M., Arasteh, H., Mashayekhi, R., Keshmiri, A., Talebizadehsardari, P., Yaïci, W. (2020). Investigation of overlapped twisted tapes inserted in a double-pipe heat exchanger using two-phase nanofluid. Nanomaterials, 10(9): 1656. https://doi.org/10.3390/nano10091656
[23] Azeez, H.L., Ibrahim, A., Ahmed, B.O., Dol, S.S., Al-Waeli, A.H., Jaber, M. (2025). Experimental investigations of heat transfer, energy, and exergy-based sustainability of a novel photovoltaic thermal system. Case Studies in Thermal Engineering, 70: 106089. https://doi.org/10.1016/j.csite.2025.106089
[24] Talib, R.N., Yasin, N.J., Nasser, M.A. (2019). The effect of external helical ribs tube on the heat transfer and pressure drop performance for multi-tube heat exchanger. IOP Conference Series: Materials Science and Engineering, 518(3): 032015. https://doi.org/10.1088/1757-899X/518/3/032015
[25] Azeez, H.L., Ibrahim, A., Ahmed, B.O., Dol, S.S., Al-Waeli, A.H., Jaber, M. (2025). Numerical and experimental investigation of heat transfer in a dimpled and petaled array tube with a coiled twisted tape and SiC nanofluid. Case Studies in Thermal Engineering, 72: 106349. https://doi.org/10.1016/j.csite.2025.106349
[26] Chang, S.W., Jan, Y.J., Liou, J.S. (2007). Turbulent heat transfer and pressure drop in tube fitted with serrated twisted tape. International Journal of Thermal Sciences, 46(5): 506-518. https://doi.org/10.1016/j.ijthermalsci.2006.07.009
[27] Chaurasiya, P.K., Heeraman, J., Singh, S.K., Verma, T. N., Dwivedi, G., Shukla, A.K. (2024). Exploring the combined influence of primary and secondary vortex flows on heat transfer enhancement and friction factor in a dimpled configuration twisted tape with double pipe heat exchanger using SiO2 nanofluid. International Journal of Thermofluids, 22: 100684. https://doi.org/10.1016/j.ijft.2024.100684
[28] Abdulrahman, R.S., Ibrahim, F.A., Dakhil, S.F. (2019). Development of paraffin wax as phase change material based latent heat storage in heat exchanger. Applied Thermal Engineering, 150: 193-199. https://doi.org/10.1016/j.applthermaleng.2018.12.149
[29] Khalil, E.E., Hwary, A., AboHedaima, S., ElShabrawy, M. (2021). Numerical investigations of heat transfer enhancement in double pipe heat exchanger using twisted tape insert. In AIAA Scitech 2021 Forum, p. 1923. https://doi.org/10.2514/6.2021-1923
[30] Alnasur, F.S., Abid Allah, N.H., Oliwier, A. (2026). Numerical investigation of hydrothermal performance enhancement using modified twisted tape having a curved and concave cross-section inserted in a horizontal tube. Journal of Applied Fluid Mechanics, 19(4): 683-696. https://doi.org/10.47176/jafm.19.4.3955
[31] Benmbarek, M.M., Moujaes, S.F. (2025). CFD analysis of heat transfer enhancement for twisted tape inserted in spirally corrugated tubes and proposal of a new vane-inserted geometry. Fluids, 10(3): 73. https://doi.org/10.3390/fluids10030073
[32] Cabello, R., Popescu, A.E.P., Bonet-Ruiz, J., Cantarell, D.C., Llorens, J. (2022). Heat transfer in pipes with twisted tapes: CFD simulations and validation. Computers & Chemical Engineering, 166: 107971. https://doi.org/10.1016/j.compchemeng.2022.107971

NOMENCLATURE

b	base length of triangle
b/D	base ratio
Cp	specific heat
C_1 and C_2	constants in ε-equation
D	diameter of tube
f	Friction factor
G_k	production of turbulent kinetic energy
$h_{(x)}$	local Convective heat transfer coefficient
h	height of triangle
k	thermal conductivity
L	length of tube
p	pitch
T	temperature
T_b	bulk temperature of the fluid
T_{out}	outlet temperature of air
T_w	wall temperature of the heated tube
Re	Reynolds number
Nu	Nusselt number
u	fluid velocity

Greek symbols

ρ	density
μ	dynamic viscosity
ε	turbulent dissipation rate
η	thermal performance factor
σ_k	turbulent Prandtl number

Abbreviations

CFD	Computational Fluid Dynamics
FVM	finite volume method
HE	heat exchanger
HEs	heat exchangers
HTE	heat transfer enhancement
PTT	perforated twisted tapes
PATT	perforated twisted tapes with alternate axis
PTTT	perforated triple twisted tape
RTT	rectangle twisted tape
TT	twisted tape
TTs	twisted tapes
TTT	triangular twisted tape
TR	twisted ratio

Subscripts

c	with twisted tape
f	fluid
m	mean
p	plain tube (without tape)